Value-based search efficiency is encoded in substantia nigra reticulata firing rate, spiking irregularity and local field potential

Abdolvahed Narmashiri[1,2], Mojtaba Abbaszadeh[2], Mohammad Hossein Nadian[2], Ali Ghazizadeh[1,2*]
[1] Bio-intelligence Research Unit, Sharif Brain Center, Electrical Engineering Department, Sharif University of Technology, Tehran, Iran
[2] School of Cognitive Sciences, Institute for Research in Fundamental Sciences (IPM), Tehran, Iran
* Corresponding: alieghazizadeh@gmail.com

Abstract

Recent results show that valuable objects can pop-out in visual search yet its neural mechanisms remain unexplored. Given the role of substantia nigra reticulata (SNr) in object value memory and control of gaze, we recorded its single unit activity while macaque monkeys engaged in efficient or inefficient search for a valuable target object among low-value objects. Results showed that efficient search was concurrent with stronger inhibition and higher spiking irregularity in target present (TP) compared to target absent (TA) trials in SNr. Importantly, the firing rate differentiation of TP and TA trials happened within ~100ms of display onset and its magnitude was significantly correlated with the search times and slopes (aka search efficiency). Time-frequency analyses of local field potential (LFP) after display onset revealed significant modulations of gamma band power with search efficiency. The greater reduction of SNr firing in TP trials in efficient search can create a stronger disinhibition of downstream superior colliculus which in turn can facilitate saccade to obtain valuable targets in competitive environments.

Keywords: value memory, visual search, search efficiency, single-unit recording, basal ganglia, substantia nigra reticulata, macaque monkey, LFP, spiking variability.

Significant statement

Most times we have to find a few relevant or highly valued objects among many objects that surround us. When our target objects are not distinct from their surroundings based on low-level features, searching for them becomes tedious and slow. Nevertheless, recent findings show that valuable objects can be found efficiently and fast if they have been repeatedly paired with reward. Our results show that the rate and pattern of spiking as well as local voltage fluctuations in the basal ganglia output which is known to control attention and saccade correlate with such value-driven search efficiency. Thus, in addition to reward learning, basal ganglia can have a role in skillful interactions and rapid detection of rewarding objects.

Introduction

Primates, including humans and monkeys, often face the challenge of quickly identifying valuable objects amongst many irrelevant or low-value objects in their surroundings. It has been long thought that visual search for targets that are not distinct from their surrounding by low-level guiding features such as color, size, or orientation should be invariably a slow and serial process requiring multiple shifts of gaze[1]. Contrary to this classical belief, we have shown that object value association especially when over-trained, can lead to efficient value-based search with minimal dependance on display size, a phenomenon we refer to as 'value-popout' [2]. However, while the efficient visual search based on low-level guiding features can be easily explained by the parallel processing of color and orientation across the visual field, the neural mechanism that allows for efficient value-based search is currently unknown.

The neural circuitry underlying object value memories has been elucidated by single-cell recording studies, implicating key regions within the basal ganglia (BG), such as the ventral putamen (vPut)[3], caudoventral globus pallidus (cvGPe)[4], caudate tail (CDt)[5,6], and substantia nigra reticulata (SNr)[7-9]. In particular, the strongest discrimination between high and low-value objects is found in SNr neurons compared to any other region BG or even the cortex[7,10]. SNr neurons exert

powerful inhibitory influence on saccades by projecting to the superior colliculus (SC) and are capable of rapidly distinguishing between objects with high and low values, within the first 100-150ms of object onsets[9]. When faced with a single valuable object, SNr neurons reduce their firing to disinhibit saccade and when encountering low value object SNr neurons increase their firing to inhibit saccades. Nevertheless, the role of SNr in visual search when multiple objects are simultaneously present and its role in enabling efficient value-based search is not previously studied.

To address this issue, we recorded single-unit activity in SNr in monkeys engaged in value-based search task with low or high search efficiency. Value-based search task consisted of trials with a single high value object among low-value objects (target-present or TP trials) and trials in which all objects where low value (target absent or TA trials). We looked at the effect of trial type and search efficiency in the first and second order statistics of firing rate as well as on local field potential power across multiple frequency bands in SNr. Briefly, results revealed that there was a stronger discrimination of TP and TA trials based on SNr firing rate and firing irregularity during efficient search. Search efficiency was also reflected and correlated firing rate changes and gamma band modulation in LFP within SNr. These findings implicate BG circuitry and in particular its output emanating from SNr in value-popout phenomenon.

Material and Methods

Subjects and surgery

In our experiments, we utilized two rhesus macaque monkeys, monkeys J and P, who were 8 and 7 years old, respectively. The experiment was conducted in accordance with ethical standards for animal care and use established by the National Institutes of Health (NIH) and after obtaining approval from the local ethics committee at the Institute for Research in Fundamental Sciences (IPM) (protocol number 99/60/1/172). Prior to the experiments, each monkey underwent sterile surgery, during which a head holder and recording chamber were implanted on their heads while they were under general anesthesia. A rectangular chamber was positioned laterally over the right hemisphere of each monkey. In a subsequent surgery, craniotomies for SNr were conducted after the monkeys learned the experimental tasks on the right hemisphere of both monkeys, following MRI confirmation of the recording chamber's location. The recording was performed using grids that had a spacing of 1 millimeter and were positioned on top of the chamber.

Recording localization

To pinpoint the location of the SNr in both monkeys, T1- and T2-weighted MRI (3 T, Prisma Siemens) were employed. T2-weighted MRI was found to be

particularly beneficial in imaging the SNr region due to its higher iron concentration[9]. Additionally, the recording chambers used for both monkeys were filled with gadolinium to enhance contrast during imaging. The standard monkey atlas (D99 atlas[11]) was transferred into each monkey's native spaces with the use of the MATres software[12] to further confirm the location of SNr in each monkey. Consequently, we ascertained the region of the SNr that was reachable for recording in each monkey via the recording chamber (Fig S1).

Stimuli

Fractal-shaped objects were utilized as visual stimuli [13], as illustrated in Fig 1A. The fractals used in the experiment consisted of four polygons that were symmetrically arranged around a central core. Each polygon had smaller polygons in front of it, and their properties such as size, edges, and color were randomly selected. On average, the diameter of the fractals subtended 4 degrees in this experiment and shown on a CRT monitor. The monkeys were exposed to a substantial number of fractals, totaling over 400, organized in sets of eight. Each set was either trained in one reward training session or in more than five reward training sessions (over-trained) and were used in visual search task subsequently.

Task control and neural recording

A customized software program written in C# (C-sharp) was used to present the task and record behavioral events and communicate with the neural data acquisition system (Cerebus Blackrock Microsystems Inc., Salt Lake City, UT, USA). Eye position was tracked at a rate of 1 kHz using an Eyelink 1000 Plus system (Ontario, Canada). Rewards were delivered in the form of apple juice diluted with water (at a 50% concentration for both monkeys), with varying amounts ranging from small (0.08 mL for both monkeys) to large (0.21 mL for both monkeys). During the experiment, the headfixed monkeys sat in a restraint chair and were presented with visual stimuli on a 21-inch CRT monitor during each experimental session.

Single-unit activity was recorded using tungsten electrodes coated with epoxy (FHC, 200 μm thickness). To prepare for each recording session, a sharp stainless steel guide tube was used to hold the electrode. The guide tube was then utilized to puncture the dura, allowing for the electrode to be cautiously inserted into the brain with the aid of an oil-driven Narishige (MO-97A, Japan) micromanipulator.

The electrical signal from the electrode was converted to a digital signal with a sampling rate of 30 kHz. Subsequently, the signals were amplified and filtered to isolate frequencies ranging from 1 Hz to 10 kHz and Blackrock's online sorting was used for online survey of available single or multi-units. The resulting spike

time data for the identified unit were then transmitted to MATLAB for generating online raster plots and peristimulus time histograms (PSTH). For the actual analysis of each session offline sorting of units using Plexon offline sorter was used (Plexon, Dallas, TX, USA). This study only considered neurons that were well-isolated and exhibited responsiveness to visual stimuli. A total of 50 neurons were recorded during both efficient or inefficient searches, comprising 28 neurons from monkey J and 22 from monkey P. To ensure consistency in our analysis, we applied the search slope criteria, as described in the results section. As a result, we utilized 48 neurons (27 from monkey J and 21 from monkey P) for further analysis, out of which 39 neurons were recorded during both types of searches (21 from monkey J and 18 from monkey P).

Neural data analysis

All neural spiking data were aligned with the visual display onset. The primary analysis window focused on the visual epoch from 100 to 400ms after the display onset. During the specified analysis period, the average firing rate was calculated separately for TP and TA trials. To assess the ability to discriminate between TP and TA trials, the area under the receiver operating characteristic curve (AUC) was calculated (termed the value AUC). The statistical significance of the AUC was determined using the Wilcoxon rank sum test for each neuron. A

cross-validation technique was used to identify the preferred value for each neuron[14].

Local field potential (LFP) Analysis

To analyze the local field potential (LFP) data, the data was down-sampled to 1 kHz and subsequently subjected to a band-pass filter to retain frequencies within the range of 0.1 to 250 Hz. Then, notch filters were applied to remove power line harmonics noise. To enhance data quality, trials with LFP amplitudes that deviated beyond 3 standard deviations from the median were determined as noisy and removed from further analysis. These preprocessing steps were carried out for each session via EEGLAB (-v2022.0). A continuous wavelet transform (CWT) was used to average across all frequencies of relevance at each time point to examine the time-frequency data. An analytical Morse wavelet was used to generate the CWT [15]. Four unique frequency bands used in this study included: alpha (8-12 Hz), beta (12-30 Hz), low-gamma (30-60 Hz), and high-gamma (60-200 Hz) ranges.

Onset detection procedure

Custom-written MATLAB functions [7,14,16] were used to identify neurons that were responsive to visual stimuli. In brief, the PSTH representing the average

firing rate of each neuron, aligned with the onset of the visual display, was computed for all trials. Then, the calculated firing rate was transformed into z-scores by comparing it to the baseline activity recorded during the period from -120 to 30ms relative to the display onset. The MATLAB function "*@findpeaks*" was used to identify the initial peak response that occurred after the display onset, with a minimum peak height threshold of 1.64, corresponding to the 95% confidence interval. The visual onset of the neuron was determined as the first valley observed before the first detected peak. The identical algorithm was employed to detect the initiation of the value signal, using the average PSTH of a specific neuron for value computation.

Object-value training task

Monkeys were trained on object values using an object saccade task, as illustrated in Fig 1B. During each trial of the task, a fixation point appeared at the center of the screen, and the subjects were instructed to maintain fixation on it. An object with a high or low value, representing either something good or bad, was presented on the screen at a location in the periphery when fixation was maintained for 200ms. The specific location was one of the eight positions that were situated at an eccentricity of 9.5 degrees. The central fixation point disappeared after a 400ms

overlap period, prompting the monkey to make a saccade towards the object stimulus and maintain gaze on it for an additional 500±100ms to deliver either a large reward (the good object) or a small reward (the bad object). After the reward was given, a varying time inter-trial interval (ITI) lasting from 1 to 1.5s began, during which a blank screen was displayed. In each training session, there were a total of 80 trials, which consisted of 16 trials (choice) where both a good object and a bad object were simultaneously displayed on the screen, as well as 64 trials (force) where each fractal was shown 8 times in a pseudo-randomized manner. The timing arrangement for both the choice trials and the force trials was identical, with the only difference being that in the choice trials, the monkey had to make a saccade to choose one of the objects to receive its corresponding reward. When the monkey completed a trial, a correct auditory voice was presented, while an error auditory voice was presented in the case of a break in fixation or an early saccade. The monkey's object value knowledge was evaluated using the results of the choice trials.

Value-driven search task

Subjects had to choose an object with high value (good) among a varying number of objects with low value (bad) in target-present (TP) trials or reject the trials by staying at or going back to the center in target-absent (TA) trials when

every object exhibited was bad[2]. Before the search task, monkeys completed a separate object value training task where they acquired knowledge regarding the object-value associations. Target-present (TP) and target-absent (TA) trials were randomly mixed with equal probability. A fixation dot was displayed on the screen to begin each trial (Fig 1E). After 400ms of fixation, the fixation point disappeared and was replaced by a display of 3, 5, 7, or 9 fractals grouped in a circular pattern with an eccentricity of 9.5°. The angle of the first fractal on the circle was uniformly chosen. For each trial, the fractals were selected in a pseudo-random manner from a set of 24 fractals, which included 12 "good" and 12 "bad" fractals. The monkey had a time of 3s to either select an object by fixating on it for 600ms (commitment time) and reject the trial by returning gaze to the center. Upon choosing an object, the reward associated with the selected object was given and the display was turned off. An ITI of 1-1.5s followed after receiving the reward. If the monkey's gaze was interrupted within a 100ms timeframe after the committing time, an error tone would be produced. However, the monkey had the liberty to shift its gaze away from an object before the commitment time had lapsed. A trial could be rejected in two ways: by maintaining gaze on the center dot for 900ms after the display onset or by returning to the center and fixating on the fixation dot for 300ms (if gaze shifted away from fixation, the fixation dot would be reactivated). Following the rejection, the next trial promptly commenced after a

delay of 400ms, and there was a 50% chance that the subsequent trial would feature a good object. In addition, monkeys had a 40% chance of obtaining a medium reward (60% of the larger reward) for the rejection trials. The purpose of this was to encourage the animals to reject TA trials if they happened to occur in a sequence and discourage them from choosing bad objects. Monkeys typically finished 240 correct trials in each search block. Subjects were well-trained in the search task prior to this experiment (> 10 search practice sessions).

One-search and two-search neurons

Each neuron was recorded with either one or two search blocks with 1-day or >5-day value trained fractals. Neurons that only had a single search block were categorized as "single-search neurons," whereas those recorded during two search blocks were labeled as "two-search neurons". In the two-search neurons, one search block involved the use of fractal sets that were over-trained, while the other block utilized fractal sets that were 1-day trained in a counter-balanced fashion.

Efficient and inefficient search sessions

The efficiency of the search sessions was determined based on the search slope during the TP trials. For each session, the search slope was calculated using MATLAB's *"@regress*" function. In the case of neurons that responded to a single

search, recording sessions with a search slope below the 40th percentile of that monkey was categorized as efficient, whereas a search slope above the 60th percentile was deemed inefficient. For two-search neurons, the session with the lower search slope was categorized as efficient, while the other session was considered inefficient if the difference in slope was greater than 10ms per item, which roughly matched the difference between the 40th and 60th percentile search slopes.

Statistical tests and significance levels

A one-way ANOVA test was conducted to determine the significance of display size on search time, accuracy, and value signal. Additionally, a two-way ANOVA test was employed to determine the effects of search efficiency and display size on the same variables. Neural firing rates were compared using t-tests for TP and TA trials in efficient and inefficient search conditions. The significance level for all statistical analyses in this study was set at $P < 0.05$.

Results

In order to understand the role of the SNr in facilitating efficient search, responses of SNr neurons were recorded while monkeys engaged in a visual search task for a high-value fractal object (methods section for more

information). The value of fractals was learned using an object-value training task prior to the search task (value training, see Fig 1A-B). A value training session was done with a set of 8 fractals, half of which were associated with low reward and the other half with high reward (referred to as bad and good fractals, respectively). The majority of trials (80%) during value learning consisted of force trials where a single fractal was shown in the periphery and after the fixation offset, the monkey had to saccade to and fixate the fractal to receive its associated reward. Choice trials (20%) interspersed during the value training were used to assess the subject's knowledge of fractal values and consisted of two diametrically presented fractals between which monkeys had to choose by making a saccade and receiving the corresponding reward (Fig 1B). It was previously shown that value-based visual search can be inefficient or efficient depending on the duration of value training that preceded search[2,17]. Thus, to create both efficient and inefficient search, The object sets underwent training for either 1-day or >5 days (over-trained fractals).

Acquisition times and choice rates during the value training sessions show robust value learning in a value learning session (Fig 1C). In both 1-day and 5-day groups the target acquisition times for good objects were significantly faster than for bad objects ($t_{220} = 11.98$, $P < 8.7381e\text{-}26$), consistent with a higher motivation to receive the large reward associated with good objects. Furthermore,

the choice rate in the 1-day and 5-day groups were high and significantly above change averaging 92% and 100%, respectively. These results show that animals had a very good knowledge of fractal values even after 1 day of value training with new fractals. Following last reward training, 1-day and 5-day fractals were used in visual search task during which neuronal responses in SNr were recorded (Fig 1D).

Rewards over-training leads to efficient search

In the search task, the monkeys were required to locate a single good fractal among multiple bad fractals in target-present (TP) trials to receive high reward. In target-absent (TA) trials where all the displayed objects were bad, they had to reject the trial by returning to the center. Rejection of a TA trial, resulted in a rapid progression to the next trial while choosing any of the bad objects was followed by the delivery of a small reward and the normal ITI to the next trial (as shown in Fig 1E). During the TP trials, monkeys received a large reward for finding the good fractal and a small reward for choosing any of the bad fractals. While fractal values in both groups were well-learned (Fig 1C), both search times and search slopes (per item of display size) were significantly smaller for overtrained fractals compared to those trained for only one day during target-present trials in both monkeys (Fig S2A). The monkeys' behavioral search slopes

varied from serial (with slopes greater than 40ms/item) to parallel (with slopes close to zero ms/item) during TP trials (Fig S2B). We grouped search performance into two types based on search slopes in TP trials with the lower 40th percentile and higher 60th percentile categorized as efficient and inefficient search, respectively.

The accuracy of good object choice in TP trials was significantly higher in efficient vs inefficient search across all display sizes (90% vs 65%, efficiency main effect: $F_{1, 372} = 223.53$, $p<0.001$, Fig. 1F). Similarly, the accuracy of trial rejection in TA trials was significantly higher in efficient vs inefficient search (Efficiency main effect: $F_{1, 372} = 85.20$, $p<0.001$). The accuracy in TP was not display-size dependent (DS main effect: $F_{3, 372} =0.31$, $p=.81$, interaction: $F_{3,372} = 0.92$, $p=0.42$, Fig. 1F) but there was a significant reduction of accuracy in both groups in TA trials in higher display sizes (DS main effect: $F_{3, 372} = 9.23$, $p<0.001$, interaction: $F_{3, 372} =0.06$, $p=0.97$, Fig. 1F).

Search time was significantly higher in inefficient vs efficient search in both TP ($F_{1,372} = 809.05$, $p<0.001$, Fig. 1F) and TA trials ($F_{1,372} = 29.93$, $p<0.001$, Fig. 1F). There was main effect in DS in both TP ($F_{3,372} = 87.98$, $p<0.001$) and TA trials ($F_{3,372,} = 60.78$, $p<0.001$). As expected from our search type definition there was a significant interaction between search type and DS in TP search slopes (interaction: $F_{3,372} = 46.09$, $p<0.001$). Additionally, there was a trending

interaction effect between search type and DS in TA trials (interaction: $F_{3,372}$ = 2.27, p=0.08). Indeed, in TA trials there was a significant reduction of search slopes from ~90ms/item in inefficient searches to ~55ms/item in efficient searches (Fig 1F).

SNr differential response to TP and TA trials is enhanced in efficient search

To investigate the role of SNr in value-based search efficiency, the activity of single neurons was recorded and contrasted in efficient and inefficient search types. Fig. 2A shows the average population response of SNr neurons in both search types in TA and TP trials and separately for each display size (Fig S3 for example neuron). As can be seen in the efficient search, there was a marked inhibition in firing in TP trials. There was a display-size dependance in firing, such that there was a larger inhibition in smaller display-sizes. This display-size dependence was significantly larger in inefficient compared to efficient search (Fig 2B). Similarly in TA trials, there was difference between efficient and inefficient search (Fig 2A, S4). While SNr neurons showed inhibition in inefficient search during TA trials, there was a slight excitation in TA trials in efficient search. Once more the display-size dependence consisted of higher firing to larger display-sizes and was significantly larger in inefficient compared to efficient search (Fig 2B).

The inhibition in TP and excitation in TA trials in efficient search resembled responses previously reported for a single good or bad object, respectively [9,16]. Notably, during inefficient search SNr showed an inhibition in both TP and TA trials consistent with the difficulty that the animal faced in determining the absence of a good object in the display.

The difference in firing to TP and TA trials in a given DS can only be due to the presence of a single good object, and we refer to this difference as the value signal (similar to our definition of the value signal for the firing difference to a single good or a single bad object[14]). The value signal was negative in SNr consistent with the response to single objects[9]. Importantly, the size of the value signal was much larger in efficient compared to inefficient search in visual epoch (t_{93}=-7.56, $p<0.001$, Fig 2C). Compared to TP or TA trial, the display-size dependence in the value signal (TP minus TA firing) was less prominent during the trial. The efficient search value signal showed higher display-size dependence compared to inefficient search early in the trial (~200ms) while later in the trial (600-800ms) the value signal in inefficient search had higher display-size dependence (Fig 2D). The onset of the value signal across the population was 105±8.27ms after display onset which is rapid and comparable to the onset of the value signal when a single object is shown [7].

To determine the TP and TA discriminability in SNr, the area under the receiver operating characteristic curve was calculated for each neuron (value AUC). Value AUCs above 0.5 indicate higher firing in TP compared to TA trials or TP-preference, and below 0.5 indicates higher firing in TA compared to TP trials or TA-preference. In both search types, the average value AUC across the population was significantly below 0.5 in neurons with both search types (Fig 2E, Efficient: AUC = 0.28, t_{38} = -15.10, P < 1.2039e-17, Inefficient: AUC = 0.44, t_{38} =-5.38, P < 3.1257e-08) and across all recorded neurons (Fig S5A, Efficient: AUC = 0.27, t_{47} = 21.40, P < 1.4782e-25, Inefficient: AUC = 0.44, t_{46} = 44.29, P < 1.3001e-35), revealing a significant TA-preference across the SNr population (X^2 = 72.15, p < 0.0001, Fig 2E, Fig S5A) . TA preference was found in 100.00% and 85.00% for Monkey J and Monkey P, respectively in efficient search while in inefficient search this number was 31.81% and 36.84% for Monkey J and Monkey P, respectively for two search neurons, as can be seen in Fig 2E (for all neurons 100.00% and 81.25% for Monkey J and Monkey P, respectively in efficient search; 35.29% and 40.00% for Monkey J and Monkey P, respectively in inefficient search, Fig S5A). The average preferred versus non-preferred responses across all neurons revealed stronger differentiation between preferred and nonpreferred values time locked to display onset in efficient search which continued to the time of saccade (Fig S5B-E).

Importantly, plotting the value signal in efficient vs inefficient search across neurons with both search types, showed that there was a significant correlation between value AUCs in the two search types for a given neuron ($r = 0.65$, $p < 0.0001$, Fig 2E). This meant that the neurons with a stronger value signal in one search type tended to have a stronger value signal in the other search type.

Critically, results also showed a significant correlation between the average value signal of the recorded neuron in the visual epoch (100-400ms post display onset) in each session and search efficiency in that session as measured by both search time and search slope in both monkeys (monkey J, search slope: $r=-0.75$, $p < 0.0001$, search time: $r=-0.60$, $p < 0.0001$, monkey P, search slope: $r=-0.64$, $p < 0.0001$, search time: $r=-0.59$, $p < 0.0001$, Fig. 2F). Therefore, one concludes that larger value signal in SNr was concurrent with faster and more efficient value-driven visual search.

SNr exhibits higher spiking variability during efficient search in TP trials

Apart from the relationship between search efficiency and SNr mean firing rate (first-order statistics), we have also looked at the changes in firing variability in SNr across the two search types (second-order statistics). The variability in firing rate can be separated into two distinct components: the first

component pertains to the trial-to-trial firing rate variability (referred to as nRV), while the second component is associated with the within-trial spiking irregularity (referred to as nSI) [18-20].

Results showed a decrease in nRV following the display onset, which was followed by a subsequent increase in nRV later in the trial consistent with earlier studies[18,19,21]. There was no significant difference in nRV during this epoch between efficient and inefficient searches (ps > 0.05, Fig 3A-B, S6). On the other hand, spiking irregularity showed a marked increase following display onset. Notably, spiking irregularity was significantly higher during efficient search in TP vs TA trials ($F_{1,372} = 11.00$, $p < 0.001$, Fig. 3A). The value signal in nSI (i.e. nSI difference in TP vs TA trials) was significantly larger in efficient vs inefficient search in visual epoch ($t_{93} = 2.71$, $P < 0.01$, Fig. 3B) but showed significant reduction in higher display-sizes for efficient search (Fig 3C). The changes in nSI and nRV in TP and TA trials were not display-size dependent in general barring some fluctuations in time (ps > 0.05, Fig 3, Fig S6).

High gamma-band power in the SNr is associated with search efficiency

Modulations in different frequency bands of the local field potential (LFP) are associated with complex cognitive processes [22,23]. Using continuous wavelet transform (CWT), we found significant changes in various LFP frequencies

within SNr during the visual search task (32 and 24 sessions in the inefficient and efficient searches, respectively). Specifically, following search display onset there was a noticeable reduction in high gamma band (100-200 Hz) power, as well as beta band (12-30 Hz) and alpha (8-12 Hz) powers (Fig 4A and Fig S7A).

Similar to the firing rate, one may calculate the value signal in LFP by subtracting the powers across frequencies in TP and TA trials (TP minus TA). Results showed a negative value signal in the gamma range following display onset (Fig. 4B, Fig S8). Notably, the reduction of high gamma value signal power was significantly stronger in efficient vs. inefficient search in the visual epoch ($F_{1,110} = 14.39$, $p < 0.0001$, Fig. 4C), but there was no main effect in DS or interaction between search type and DS (Interaction: $F_{3,110} = 0.66$, $p=0.58$, DS main effect: $F_{3,110} = 0.33$, $p = 0.80$). There was no significant difference in the value signal across alpha, beta, and low gamma bands between efficient and inefficient search in the visual epoch (ps > 0.05, Fig S8).

Similar to the value signal in firing rate, there was a significant negative correlation between the value signal during the visual epoch in high gamma and search slope in both monkeys and a trend for negative correlation with search time (monkey J, $r=-0.54$, $p < 0.01$; monkey P: $r=-0.42$, $p < 0.05$, Fig. 4D). No significant relationship in the visual epoch was observed in alpha, beta, or low gamma bands (except for alpha band in monkey J for search slope: $r=-0.49$, p <

0.01, and search time: r=-0.38, $p < 0.05$, Fig S9). These suggest that among frequency bands in SNr, high gamma signal encodes value signal and is a good correlate of search efficiency in the visual epoch. While the alpha band power in a later epoch (500-800ms) also showed a significant correlation with search efficiency given the fact that mean saccade times in the search task are ~700ms this correlation would be too late to causally affect the search time.

Discussion

While the role of overtrained value as a high-level guiding feature in visual search has been recently recognized [2,24], its underlying neural mechanism remains unknown. Given the role of SNr in control of visual attention and saccades[25] as well as in object value memory[7,9,16], we investigated its role in value-based visual search efficiency by recording neural activity of a single neuron in both efficient and inefficient search with varying display sizes. The neurons in the SNr exhibited stronger inhibition during TP (target present) trials in comparison to TA (target absent) trials (Fig 2A, Fig S3-S4). Results show that the firing rate in TP and TA trials in inefficient search was more display-size dependent. Importantly, the firing difference to TP and TA trials (firing value signal) was significantly stronger in efficient search and there was a significant correlation between the strength of this value signal and search efficiency across sessions (Fig 2). In addition to the firing

rate, in efficient visual search was concurrent with higher spiking irregularity following the display onset during TP trials (Fig 3). LFP signals in SNr were also affected by search efficiency. In particular, high gamma power showed a larger reduction in TP trials during efficient search and this power modulation was correlated with search efficiency in a given session (Fig 4).

Efficient search for valuable objects is vital for survival in the wild. Animals explore their environment, encountering objects of varying values. Objects are considered high value and preferred, based on their past learned associations with reward and their effect on enhancing the animal's competitive fitness. Objects associated with rewards tend to capture gaze and attention independent of low-level salience [26-29]. Our results showed that object value can also result in efficient object search [2]. Recent evidence shows that areas within BG (posterior BG circuitry) play a key role in formation and retention of object value memories and in directing gaze toward valuable objects [3,4,6,9,30] modulated by inputs from a special class of dopaminergic neurons in the SNc[31]. The output of BG emanating from SNr impacts gaze direction via projection to the SC[32,33]. Value signals in the posterior BG circuit can also affect cortical regions through thalamocortical connections, facilitating quick identification of valuable objects[34,35]. Given the inhibitory role of SNr on saccades, the stronger reduction of its neural firing in TP

trials during efficient search should result in greater disinhibition of SC neurons to allow rapid gaze shift toward detected targets [36].

We have also looked at the changes in the neural variability using a recent method that allows parsing two components related to firing rate variability (nRV) and spiking irregularity (nSI)[18,37]. The temporal dynamics of nRV and nSI in SNr in the search task was similar to its pattern in passive viewing of good and bad objects [18]. Consistent with previous reports[21], we found a transient reduction of firing rate variability (nRV) following display onset but unlike the finding in some cortical areas [19], this component of variability was not display-size dependent. nRV was not modulated by search efficiency either. Unlike nRV, spiking irregularity (nSI) was found to be affected by search efficiency. In particular, efficient search was associated with higher spiking irregularity in the SNr during target-present trials compared to target-absent trials. While our understanding of the computational and behavioral impact of spiking irregularity is nascent, there is growing evidence implicating spiking irregularity in information coding and for feasibility of its decoding in downstream areas [38]as well as its role for affecting behavior[39]. In particular it is shown that bursting can contributes to higher spiking irregularity in SNr [18] and that bursting increases the reliability of synaptic transmission [40]. It remains to be seen whether higher spiking irregularity during

efficient search indeed facilitates detection and saccade to good objects via a more effective information transmission to SC for instance.

Despite a large number of studies on SNr neural firing in value-related tasks there is surprisingly little work on the LFP signals in this region especially using event-related time-frequency analysis. This study provides the first systematic analysis of LFP in a complex value-based task in SNr. Time-frequency analysis of LFP showed clear reduction of power in high gamma band (100-200 Hz), beta band (12-30 Hz) and alpha band (8-12 Hz) time-locked to display onset in both TP and TA trials. The power reduction was more prominent in TP compared to TA trials in efficient search in high gamma band. This high gamma value signal was correlated with improved search slopes across sessions (Fig 4). While the origin and significance of LFP signals in cortical and subcortical regions can be very diverse [41], it is generally thought that while high gamma band modulation reflects local computations and carry significant mutual information with the spikes in a region, low frequency band codes information independent from firing rates carrying mostly afferent information to the region [42-44]. This interpretation suggests the intriguing possibility that given the presence of value signal in high gamma and its absence in lower frequencies, rather than being fully determined by inputs to SNr, the efficient detection of high value target is computed withing SNr neurons. The enhanced value signal in high gamma band during efficient value-based search

has been recently reported in ventrolateral prefrontal cortex (vlPFC) [17]. vlPFC and SNr are known to participate in cortico-basal ganglia loops and to commonly encode object value memories [7]. Overall, these findings suggest that gamma-band activity in the SNr may play a critical role in visual search, potentially serving as a marker for target detection and attentional selection.

The current findings suggest that the disinhibition of SC by SNr can enable efficient identification of high-value objects. The results revealed a link between the strength of the value signal in the firing rate and gamma band activity in the SNr and the efficiency of visual search for objects. The relatively large size of receptive fields in SNr [7]allows for parallel processing of contralateral visual hemifield to indicate presence of a valuable target. It is then possible for vlPFC which is sensitive to object value and has a more localized receptive field [7] to direct gaze toward the exact location of the valuable target [17]. Additional research is needed to establish and differentiate the role of cortical and subcortical areas involved in 'value pop-out' during visual search for objects.

Acknowledgments

We thank M. Khorasani, A. Shabani, and G. Sadeghian, for technical assistance in monkey care and Ghazizadeh lab for helpful cooperation (S.

Meghdadi, A. Panjehpoor, M. Khademian, A. Mirzadeh, Nikkozadeh and Mokhtari).

Funding: This work was financially supported by the Cognitive Science and Technology Council of Iran (CSTC) (Grant No. 14071/100/d).

Competing interests: The authors declare that they have no competing interests.

Data and materials availability: All data needed to evaluate the conclusions in the paper are present in the paper and/or the Supplementary Materials. Additional data related to this paper may be requested from the authors.

References

1 Wolfe, J. M. Guided Search 6.0: An updated model of visual search. *Psychonomic Bulletin & Review* **28**, 1060-1092 (2021).

2 Ghazizadeh, A., Griggs, W. & Hikosaka, O. Object-finding skill created by repeated reward experience. *Journal of vision* **16**, 17-17 (2016).

3 Kunimatsu, J., Maeda, K. & Hikosaka, O. The caudal part of putamen represents the historical object value information. *Journal of Neuroscience* **39**, 1709-1719 (2019).

4 Kim, H. F., Amita, H. & Hikosaka, O. Indirect pathway of caudal basal ganglia for rejection of valueless visual objects. *Neuron* **94**, 920-930. e923 (2017).

5 Yamamoto, S., Kim, H. F. & Hikosaka, O. Reward value-contingent changes of visual responses in the primate caudate tail associated with a visuomotor skill. *Journal of Neuroscience* **33**, 11227-11238 (2013).

6 Kim, H. F. & Hikosaka, O. Distinct basal ganglia circuits controlling behaviors guided by flexible and stable values. *Neuron* **79**, 1001-1010 (2013).

7 Ghazizadeh, A. & Hikosaka, O. Common coding of expected value and value uncertainty memories in the prefrontal cortex and basal ganglia output. *Science Advances* **7**, eabe0693 (2021).

8 Ghazizadeh, A. & Hikosaka, O. Salience memories formed by value, novelty and aversiveness jointly shape object responses in the prefrontal cortex and basal ganglia. *Nature communications* **13**, 1-14 (2022).

9 Yasuda, M., Yamamoto, S. & Hikosaka, O. Robust representation of stable object values in the oculomotor basal ganglia. *Journal of Neuroscience* **32**, 16917-16932 (2012).

10 Hikosaka, O., Kim, H. F., Yasuda, M. & Yamamoto, S. Basal ganglia circuits for reward value–guided behavior. *Annual review of neuroscience* **37**, 289-306 (2014).

11 Reveley, C. *et al.* Three-dimensional digital template atlas of the macaque brain. *Cerebral cortex* **27**, 4463-4477 (2017).
12 Nadian, M. H., Farmani, S. & Ghazizadeh, A. A novel methodology for exact targeting of human and non-human primate brain structures and skull implants using atlas-based 3D reconstruction. *Journal of Neuroscience Methods*, 109851 (2023).
13 Miyashita, Y., Higuchi, S.-I., Sakai, K. & Masui, N. Generation of fractal patterns for probing the visual memory. *Neuroscience research* **12**, 307-311 (1991).
14 Ghazizadeh, A., Hong, S. & Hikosaka, O. Prefrontal cortex represents long-term memory of object values for months. *Current Biology* **28**, 2206-2217. e2205 (2018).
15 Aguiar-Conraria, L. & Soares, M. J. The continuous wavelet transform: A primer. (NIPE-Universidade do Minho, 2011).
16 Ghazizadeh, A. & Hikosaka, O. Salience memories formed by value, novelty and aversiveness jointly shape object responses in the prefrontal cortex and basal ganglia. *Nature Communications* **13**, 6338 (2022).
17 Abbaszadeh, M., Panjehpour, A., Alemohammad, S. M. A., Ghavampour, A. & Ghazizadeh, A. Prefrontal Cortex Encodes Value Pop-out in Visual Search. *bioRxiv*, 2023.2001. 2027.525832 (2023).
18 Fayaz, S., Fakharian, M. A. & Ghazizadeh, A. Stimulus presentation can enhance spiking irregularity across subcortical and cortical regions. *PLoS Computational Biology* **18**, e1010256 (2022).
19 Churchland, A. K. *et al.* Variance as a signature of neural computations during decision making. *Neuron* **69**, 818-831 (2011).
20 Churchland, M. M. & Abbott, L. Two layers of neural variability. *Nature neuroscience* **15**, 1472-1474 (2012).
21 Churchland, M. M. *et al.* Stimulus onset quenches neural variability: a widespread cortical phenomenon. *Nature neuroscience* **13**, 369-378 (2010).
22 Buzsaki, G. & Draguhn, A. Neuronal oscillations in cortical networks. *science* **304**, 1926-1929 (2004).
23 Buzsáki, G. & Wang, X.-J. Mechanisms of gamma oscillations. *Annual review of neuroscience* **35**, 203-225 (2012).
24 Wolfe, J. M. Visual search: How do we find what we are looking for? *Annual review of vision science* **6**, 539-562 (2020).
25 Hikosaka, O., Nakamura, K. & Nakahara, H. Basal ganglia orient eyes to reward. *Journal of neurophysiology* **95**, 567-584 (2006).
26 Anderson, B. A., Laurent, P. A. & Yantis, S. Value-driven attentional capture. *Proceedings of the National Academy of Sciences* **108**, 10367-10371 (2011).
27 Hickey, C., Chelazzi, L. & Theeuwes, J. Reward changes salience in human vision via the anterior cingulate. *Journal of Neuroscience* **30**, 11096-11103 (2010).
28 Libera, C. D. & Chelazzi, L. Visual selective attention and the effects of monetary rewards. *Psychological science* **17**, 222-227 (2006).
29 Towal, R. B., Mormann, M. & Koch, C. Simultaneous modeling of visual saliency and value computation improves predictions of economic choice. *Proceedings of the National Academy of Sciences* **110**, E3858-E3867 (2013).
30 Yamamoto, S., Monosov, I. E., Yasuda, M. & Hikosaka, O. What and where information in the caudate tail guides saccades to visual objects. *Journal of Neuroscience* **32**, 11005-11016 (2012).
31 Kim, H. F., Ghazizadeh, A. & Hikosaka, O. Dopamine neurons encoding long-term memory of object value for habitual behavior. *Cell* **163**, 1165-1175 (2015).

32 Hikosaka, O. & Wurtz, R. H. Visual and oculomotor functions of monkey substantia nigra pars reticulata. IV. Relation of substantia nigra to superior colliculus. *Journal of neurophysiology* **49**, 1285-1301 (1983).
33 Hikosaka, O. *et al.* Direct and indirect pathways for choosing objects and actions. *European Journal of Neuroscience* **49**, 637-645 (2019).
34 Middleton, F. A. & Strick, P. L. Basal-ganglia 'projections' to the prefrontal cortex of the primate. *Cerebral cortex* **12**, 926-935 (2002).
35 Ghazizadeh, A., Griggs, W., Leopold, D. A. & Hikosaka, O. Temporal–prefrontal cortical network for discrimination of valuable objects in long-term memory. *Proceedings of the National Academy of Sciences* **115**, E2135-E2144 (2018).
36 Basso, M. A. & Wurtz, R. H. Modulation of neuronal activity by target uncertainty. *Nature* **389**, 66-69 (1997).
37 Vinci, G., Ventura, V., Smith, M. A. & Kass, R. E. Separating spike count correlation from firing rate correlation. *Neural computation* **28**, 849-881 (2016).
38 Gallinaro, J. V. & Clopath, C. Memories in a network with excitatory and inhibitory plasticity are encoded in the spiking irregularity. *PLoS Computational Biology* **17**, e1009593 (2021).
39 Doron, G., Von Heimendahl, M., Schlattmann, P., Houweling, A. R. & Brecht, M. Spiking irregularity and frequency modulate the behavioral report of single-neuron stimulation. *Neuron* **81**, 653-663 (2014).
40 Zeldenrust, F., Wadman, W. J. & Englitz, B. Neural coding with bursts—current state and future perspectives. *Frontiers in computational neuroscience* **12**, 48 (2018).
41 Buzsáki, G., Anastassiou, C. A. & Koch, C. The origin of extracellular fields and currents—EEG, ECoG, LFP and spikes. *Nature reviews neuroscience* **13**, 407-420 (2012).
42 Khawaja, F. A., Tsui, J. M. & Pack, C. C. Pattern motion selectivity of spiking outputs and local field potentials in macaque visual cortex. *Journal of Neuroscience* **29**, 13702-13709 (2009).
43 Rasch, M. J., Gretton, A., Murayama, Y., Maass, W. & Logothetis, N. K. Inferring spike trains from local field potentials. *Journal of neurophysiology* **99**, 1461-1476 (2008).
44 Belitski, A. *et al.* Low-frequency local field potentials and spikes in primary visual cortex convey independent visual information. *Journal of Neuroscience* **28**, 5696-5709 (2008).

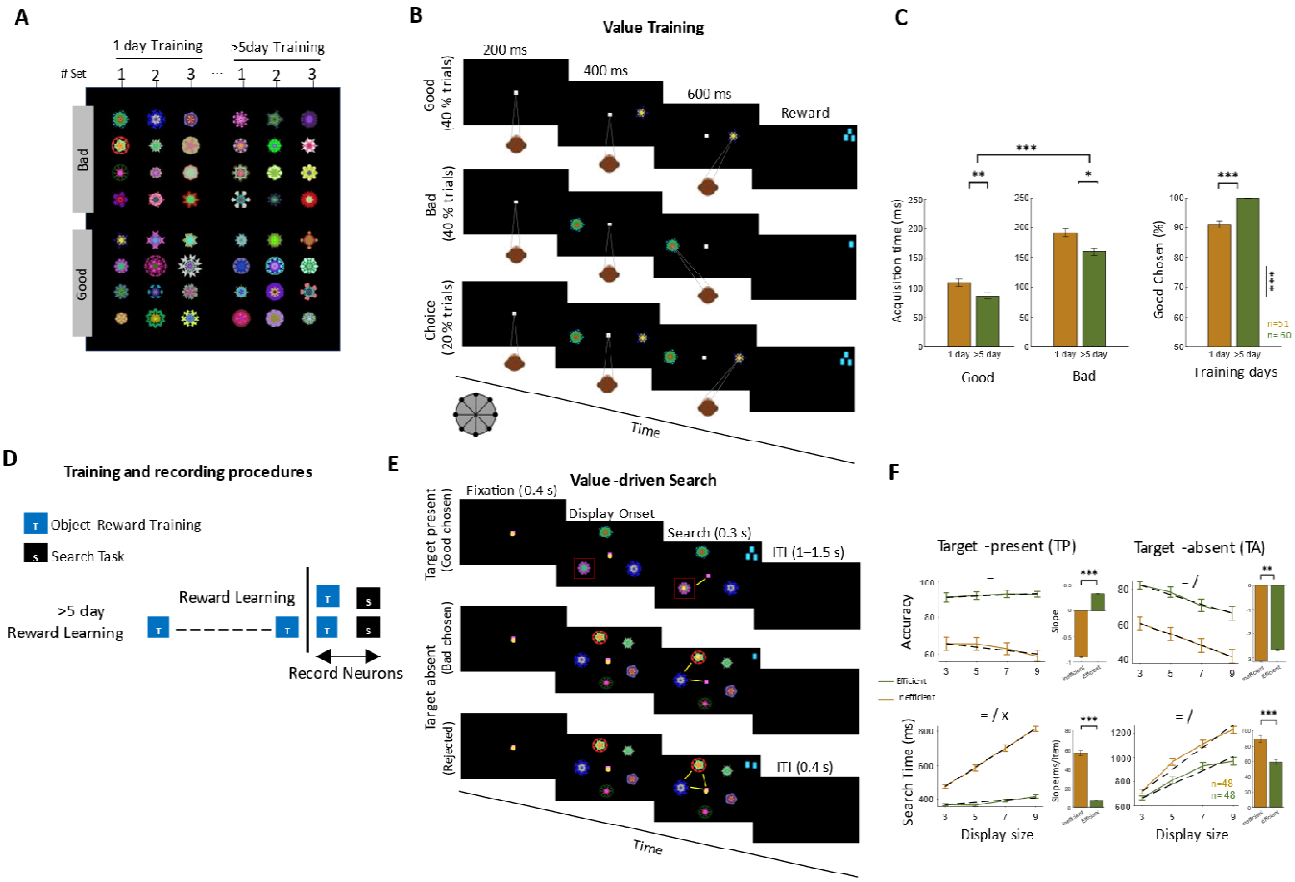

Fig 1. Value-based search paradigm and stimuli. A) The monkeys were trained with >400 fractal objects, which were divided into sets of eight, consisting of four fractals with high reward and four with low reward associations. These sets of fractals were subjected to value-based training, which lasted either for 1 day or >5 days. B) During the value training phase, the subjects participated in two types of trials: forced and choice trials which were intermixed. In forced trials, a single object (either good or bad) appeared randomly in one of 8 locations on the screen after a central fixation point, and the subjects had to make a saccade toward the presented object to receive a reward. In choice trials, two fractals (one good and one bad) appeared randomly in two of the 8 locations on the screen after a central fixation point, and the subjects had to choose one of the presented fractals to deliver the reward. C) The performance of the monkeys in the value training task. The time taken to acquire good objects and bad objects in forced trials (left two plots). The percentage of good object choice in choice trials (right plot) separately for objects that were trained for 1 day and objects that were trained for >5 days. D) Search task is done using distinct sets of reward-biased fractals with varying training durations (1-day and >5days) E) The search task consisted of target-present (TP) and target-absent (TA) trials. In each trial, a varying number of fractals (3, 5, 7, or 9) were displayed at equal distance on a circle 9.5° eccentricity. In TP trials, only one of the displayed fractals was good, while in TA trials, all of the displayed fractals were bad. The monkey could get large reward after finding and fixating the good object in TP trials and could proceed rapidly to the next trial by rejecting TA trials. F) Percentage of trials finding the good objects in TP trials and in rejecting the trial in

TA trials (accuracy, top row) and search time taken to find good objects in TP or reject the trial in TA trials (bottom row), for both efficient and inefficient. The dotted line represents the linear fit and the inset bar plots indicate slopes. The symbols =, /, and x represent the main effects of search efficiency, display size, and their interaction, respectively. The symbols *, **, and *** indicate statistical significance levels at $p < 0.05$, $p < 0.01$, and $p < 0.001$, respectively here and thereafter.

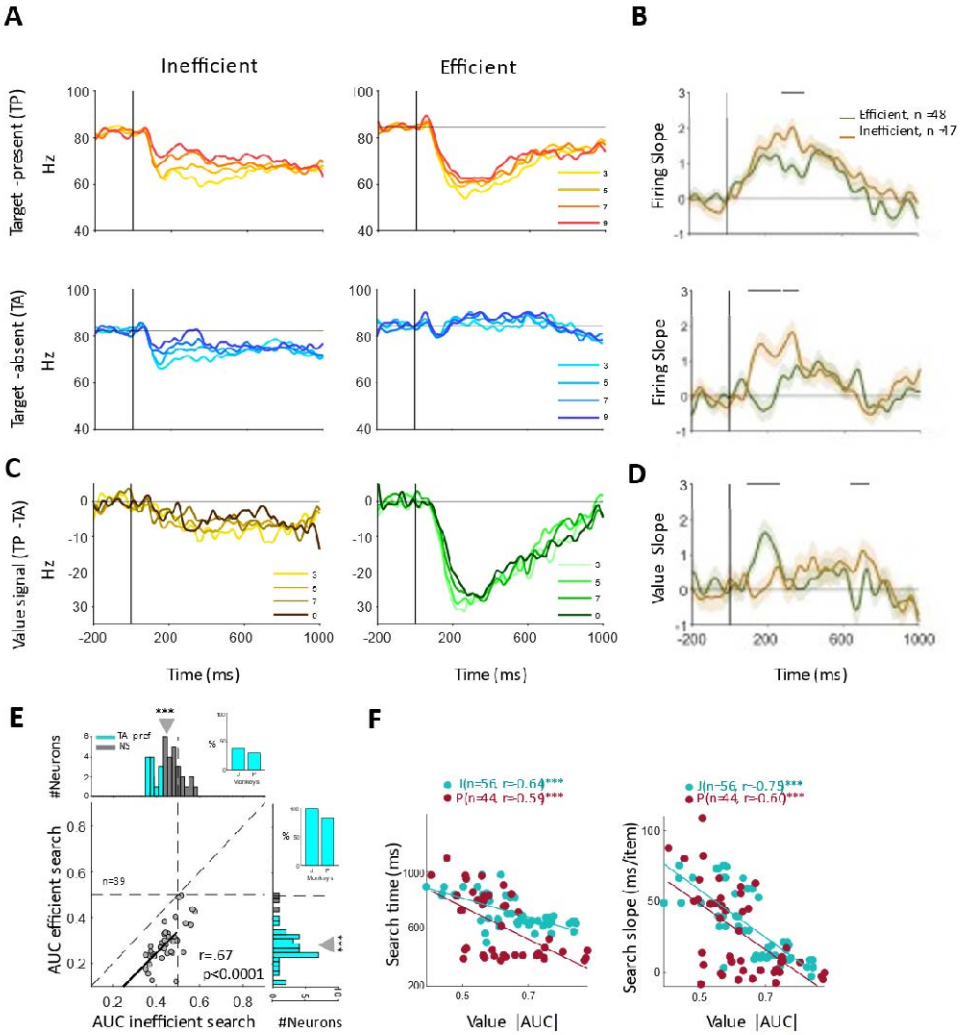

Fig 2. The SNr differential neural firing in TP and TA trials correlates with search efficiency. A) The population average firing time-locked to display onset separately for display sizes in TP and TA trials. Mean firing rate for the baseline period (-120 to 30ms) is indicated by a black horizontal line. B) The firing slope as a function of display size in inefficient vs. efficient searches in TP (top row) and TA (bottom row) trials. Lines above the PSTHs indicate significance at the $p < 0.01$ in 25ms bins. C) The firing difference between TP and TA signals (firing value signal), separately for each display size. D) Same format as B but for value signal slope as a function of display size. E) Value signal AUC scatter for neurons in inefficient vs efficient search. The linear fit is shown as a solid dark line. Marginal value AUC histograms are shown and neurons with significant value AUC are color-coded (TA-preferred, significant AUC < 0.5 and nonsignificant NS neurons). The insets show the percentage of TA-preference neurons for both monkeys. F) Scatter plots showing search time and search slopes in TP trials as a function of the absolute value AUC in firing rate across sessions for the two monkeys.

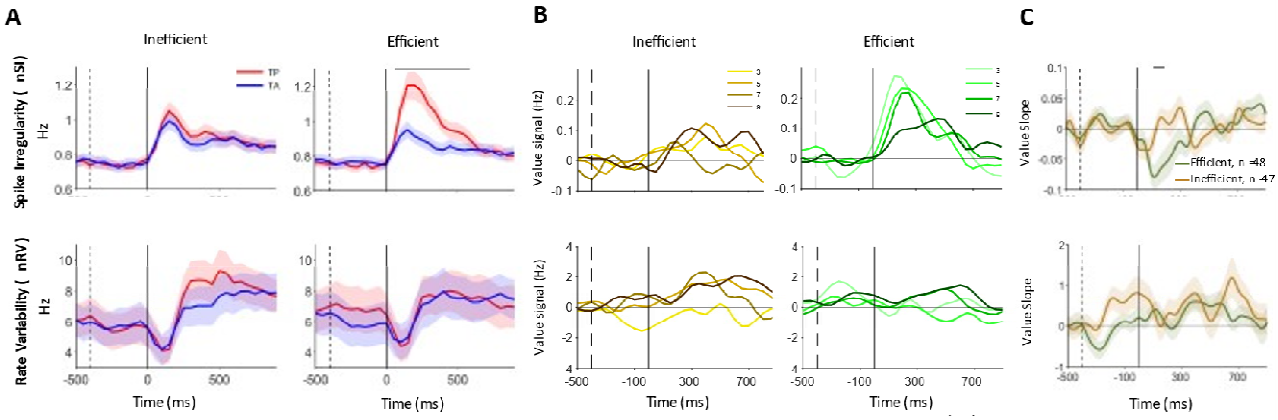

Fig 3. Spiking variability in TP trials during efficient searches. A) Population average collapsed across all display sizes in the TP trials (red) and the TA trials (blue) for the inefficient (left) and efficient (right) searches for spiking variability (nSI, top), and rate variability (nRV, bottom). B) The difference between TP and TA trials separately for display sizes for inefficient (left) and efficient (right) searches for nSI (top), and nRV (bottom). C) The value signal slope as function of display size across time for nSI (top), and nRV (bottom) for efficient and inefficient searches. Lines above the PSTHs indicate significance at the $p < 0.01$ level.

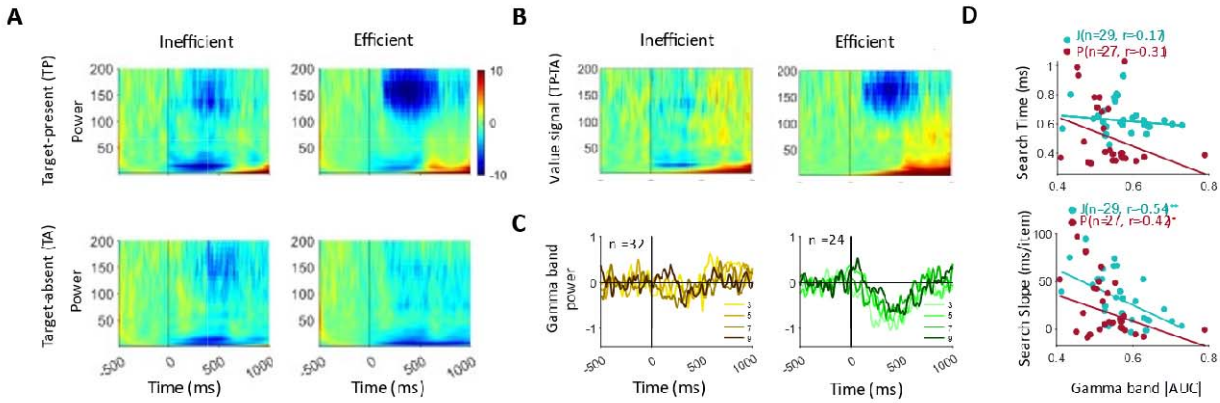

Fig 4. High gamma band power modulations in efficient vs inefficient search. A) Changes in LFP power ($20\log_{10}$) time-locked to display onset, spanning the frequency range of 0-200 Hz, averaged across display sizes for target-present (TP) trials (top) and target-absent (TA) trials (bottom) in inefficient and efficient search. The color code represents the changes in LFP power compared to the average baseline power (-500-0ms). B) The difference in LFP power between TP and TA trials, during inefficient and efficient search (LFP value signal). C) The value signal of gamma-band power over time separately for each display size in inefficient and efficient searches. D) Scatter plots showing search time and search slopes in TP trials as a function of the absolute value AUC in gamma band power across sessions for the two monkeys.

Supplementary Figures

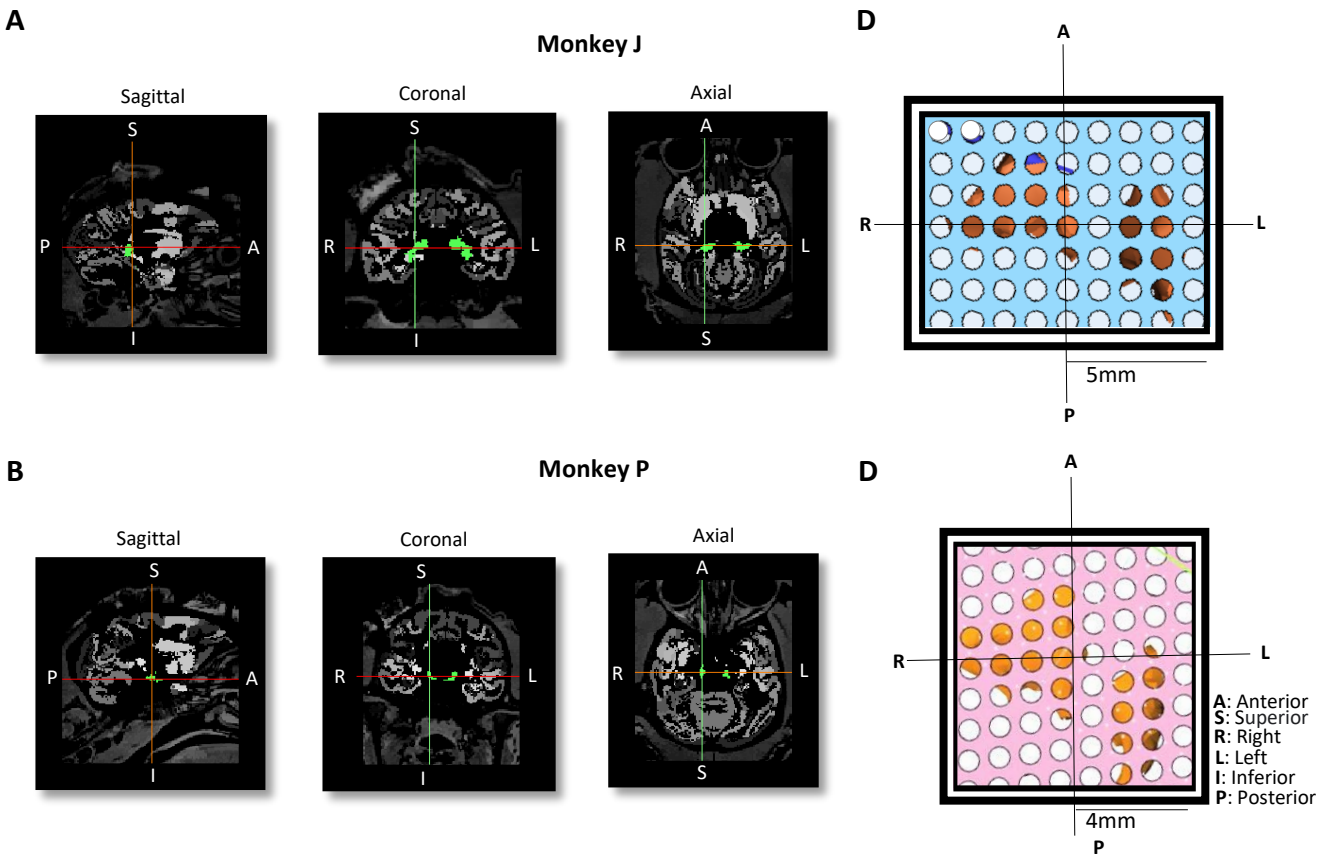

Fig S1. Targeting SNr and recording sites. A, B) Sagittal, coronal, and axial views of the SNr region of two monkey brains that have been registered standard brain atlas (D99). C, D) In the parallel view to the chamber, neural recording sites are visible for both J and P monkeys. These recording sites are registered on the monkey brain atlas and the SNr region can be seen through the recording gird. Each hole in the image represents a neural recording site.

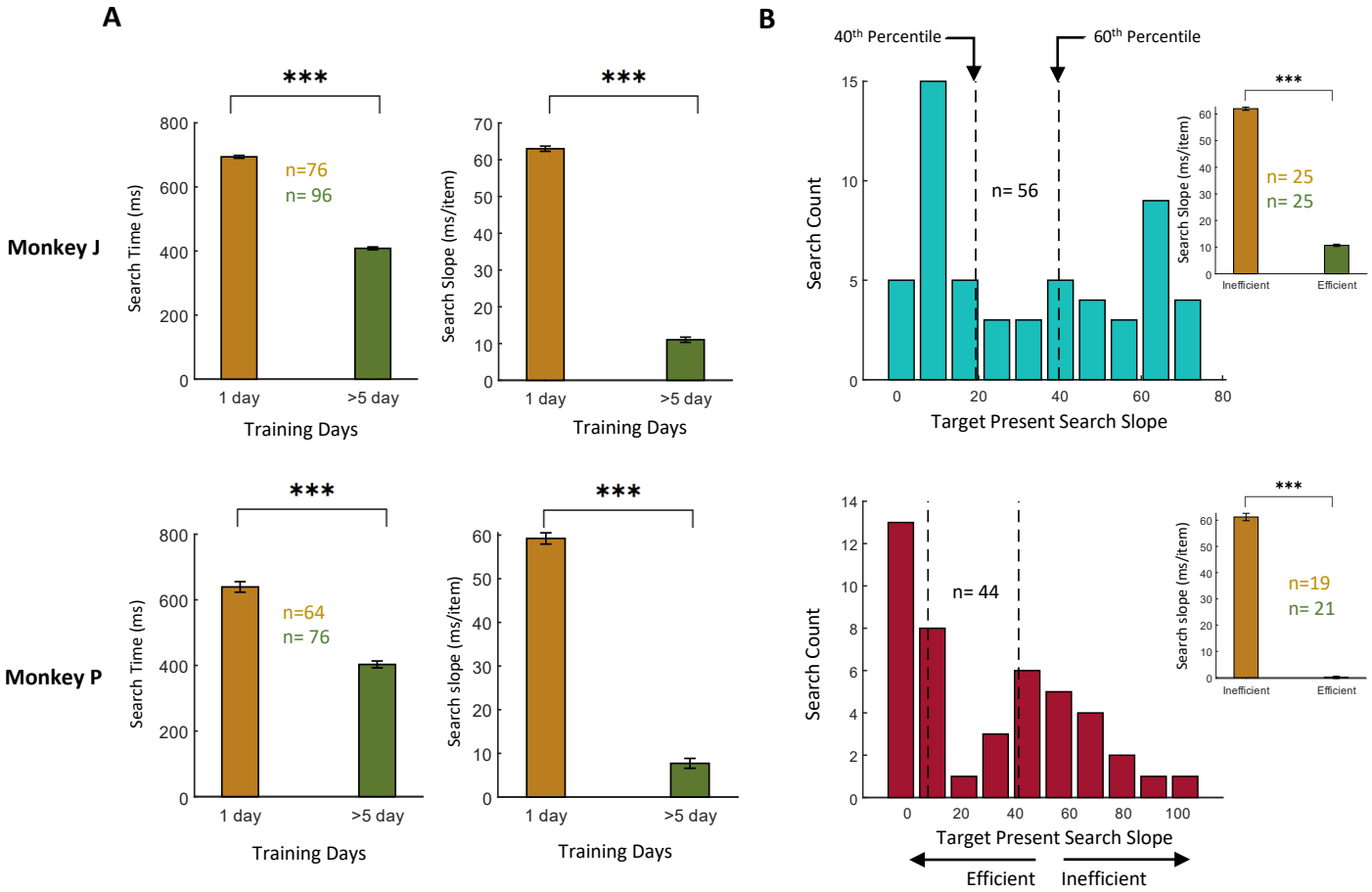

Fig S2. Behavioral performance of monkeys in value-based visual search. A) Search time and search time slope, respectively, for one-day trained and more than five-day trained fractal sets in TP trials for Monkey J (top) and Monkey P (bottom). B) Search time slope distribution for Monkey J (top) and Monkey P (bottom) in TP trials for all sessions. The x-axis shows the search time slope, and the y-axis indicates the number of sessions. Sessions with search slopes in the lower 40th percentile or higher 60th percentile were grouped as efficient and inefficient, respectively, for each monkey for subsequent analysis. Insets show the average search time slope for inefficient (orange) and efficient (green) search sessions for each monkey based on the percentile definition. The symbols *, **, and *** indicate statistical significance levels at $p < 0.05$, $p < 0.01$, and $p < 0.001$, respectively.

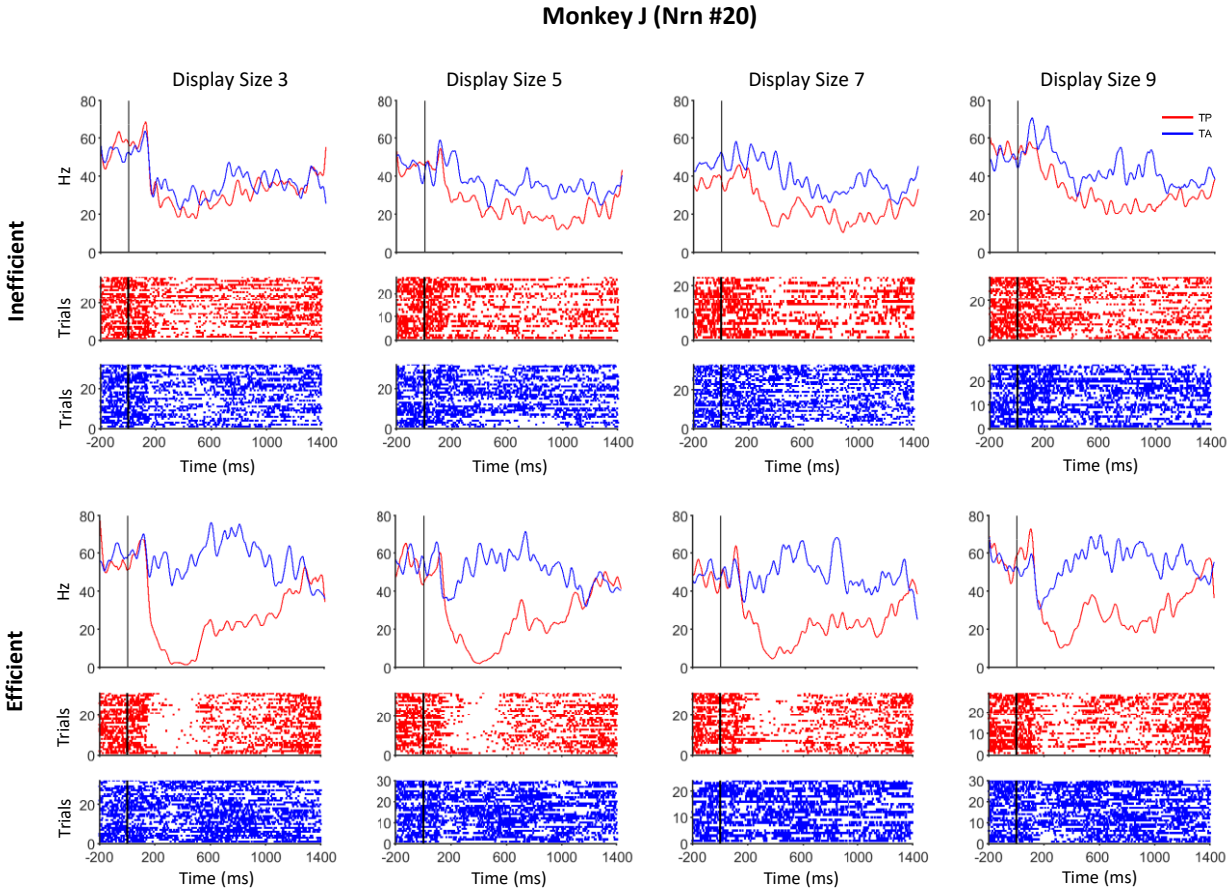

Fig S3. Firing rate response to target-present (TP) and target-absent (TA) trials during efficient and inefficient searches in an example SNr neuron. A) Peristimulus time histograms (PSTH) and raster plots in TP (shown in red) and TA (shown in blue) trials, time-locked to display onset are shown. The display sizes of 3, 5, 7, and 9 are shown in separate columns and inefficient and efficient search types are shown in top and bottom rows.

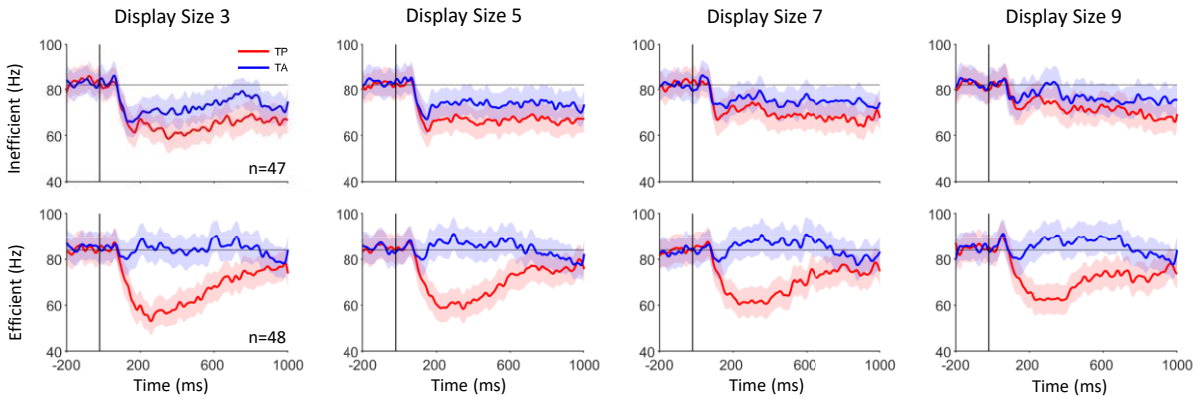

Fig S4. The average PSTH across SNr neurons in target-present (TP) and target-absent (TA) trials during efficient and inefficient searches separately for each display size. The TP and TA trials are indicated in red and blue colors, respectively. The onset time of the stimulus is denoted by vertical solid lines. The mean firing rate for the baseline period (-120 to 30ms) is indicated by a horizontal line.

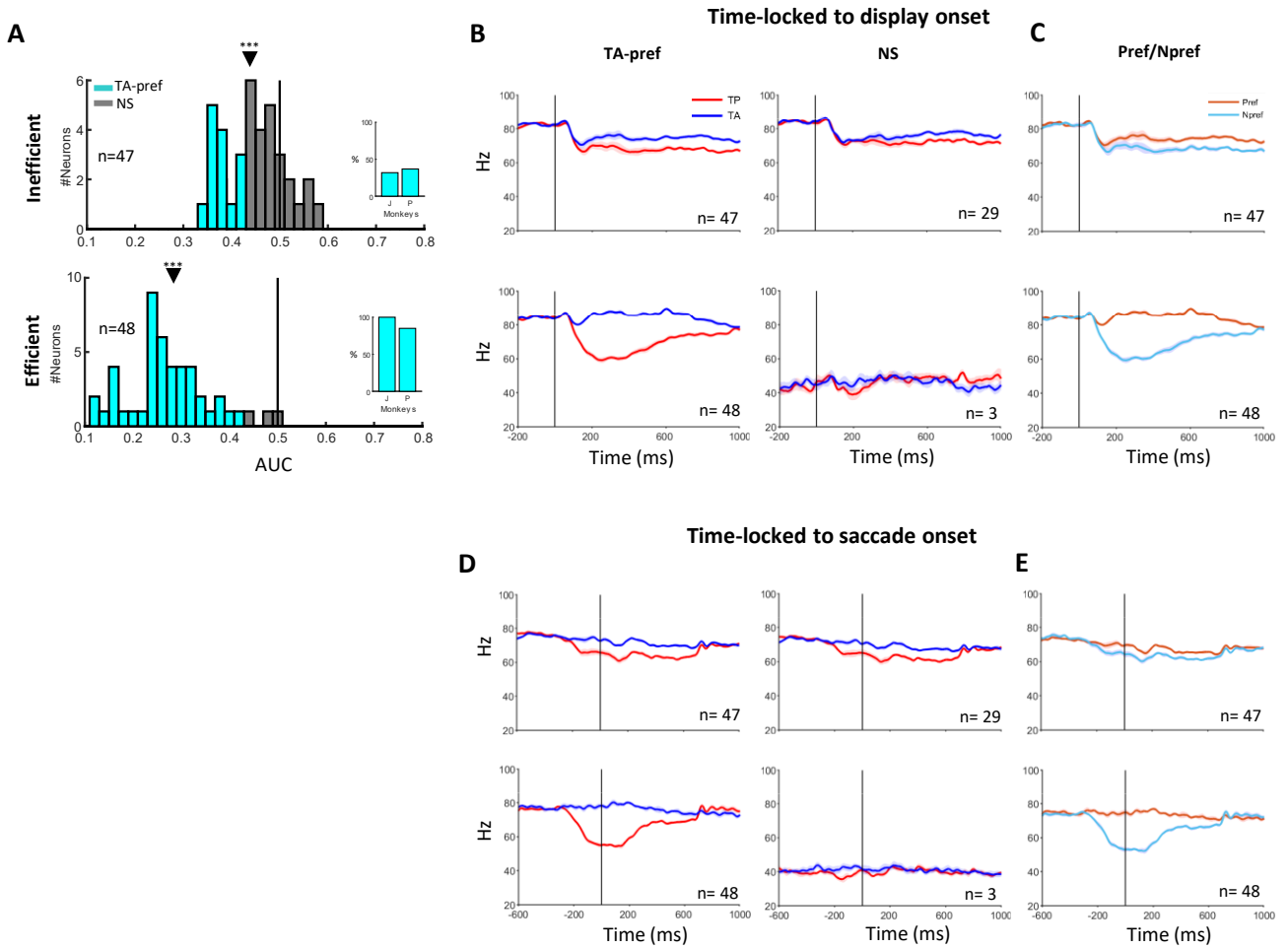

Fig S5. The value preference in SNr neurons in inefficient and efficient search. A) Histogram of the firing value AUC for inefficient (top) and efficient (bottom) search for all neurons (with single or two searches). The histogram used light blue and gray colors to indicate the TA-preferred (TA-pref, significant AUC < 0.5) and nonsignificant (NS) neurons, respectively. Mean of the histogram distribution is marked with an arrow on top. Insets were added to show the percentage of TA-pref neurons for both monkeys in each search type. B) Population average PSTH time locked to display onset for TA-pref and NS neurons in the inefficient (top) and efficient (bottom) searches. C) Population average PSTH time-locked to display onset for preferred versus non-preferred response of neurons (preference determined by cross validation, see methods) in inefficient (top) and efficient (bottom) searches. D-E) Same format as B-C, but time-locked to saccade onset.

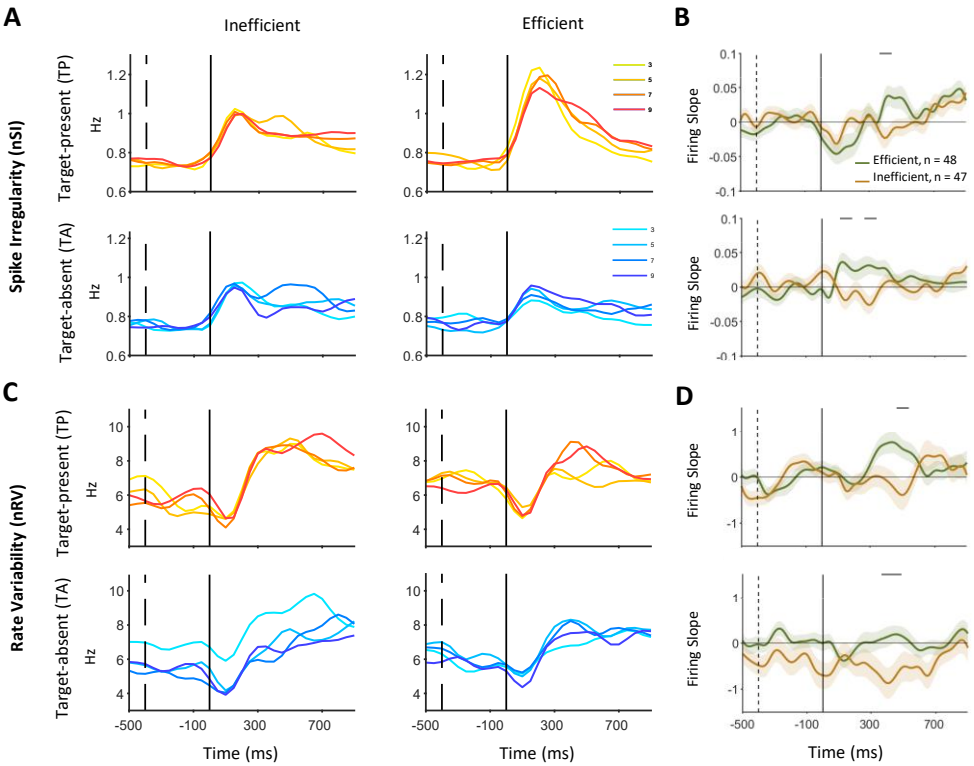

Fig S6. nSI and nRV in SNr neurons in TP and TA trials and for inefficient and efficient searches. A) Population average nSI collapsed across display sizes for the inefficient and efficient searches and for the TP trials and the TA trials separately for each display size B) The nSI slope in inefficient vs. efficient searches in TP and TA trials as a function of display size. Lines above the PSTHs indicate significance at the $p < 0.01$ in 25ms bins. C-D) Same format as A-B, but for nRV.

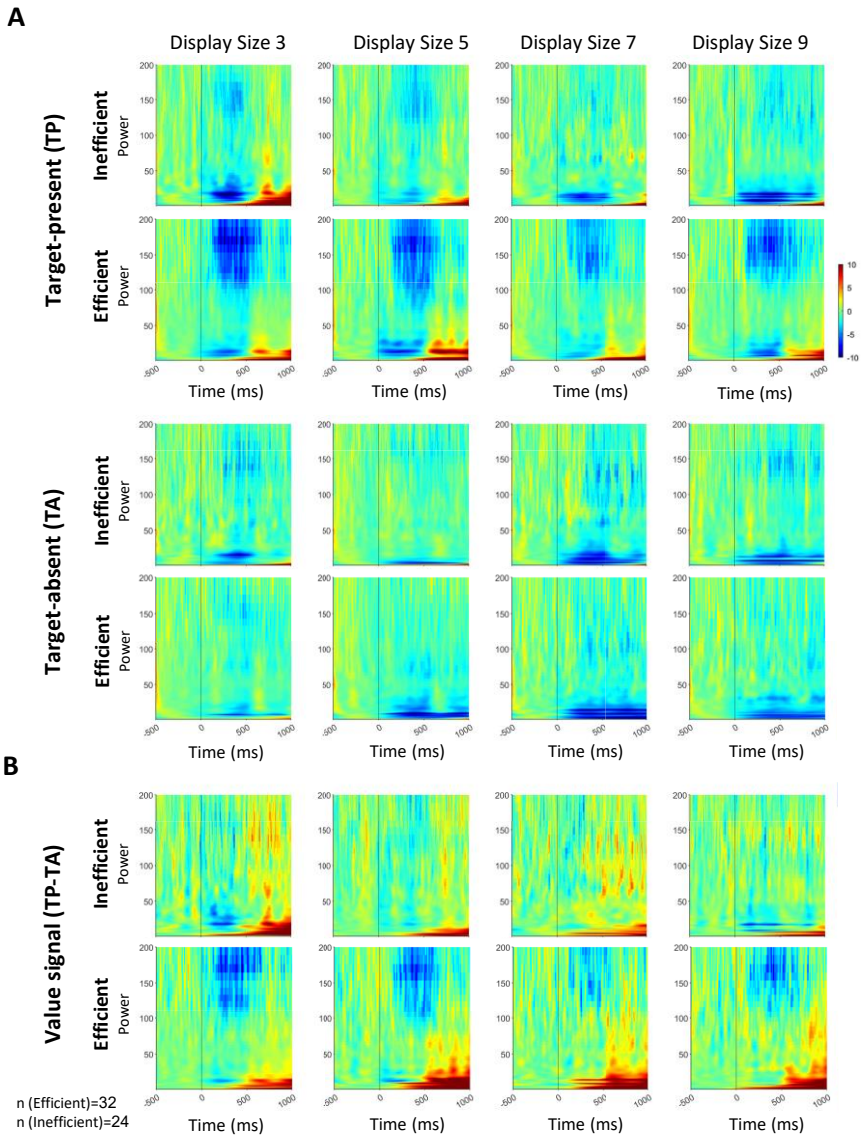

Fig S7. LFP power modulation time locked to display onset in inefficient and efficient searches using time-frequency analysis (CWT). A) Similar to Fig 4A, but shown separately for each display size. B) Same to Fig. 5B but shown separately for each display size.

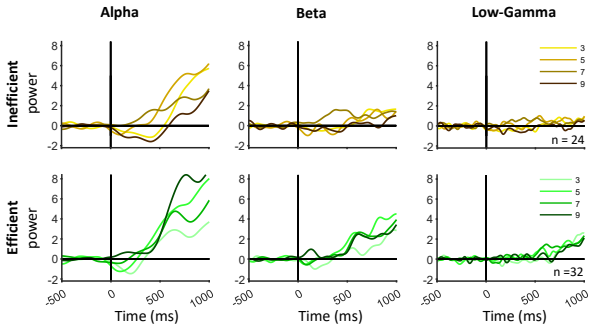

Fig S8. Value signals in alpha, beta, and low gamma LFP frequency bands during the efficient and inefficient search. A) Value signal in the alpha (left), beta (middle), and low gamma (right) frequency bands for different display sizes in LFP sessions of inefficient and efficient searches similar to Fig 4C.

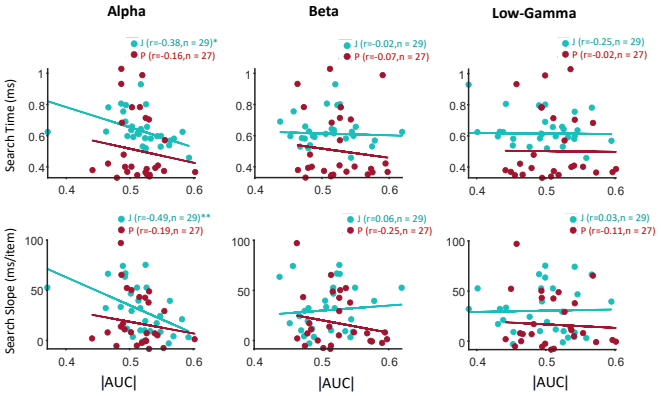

Fig S9. The correlation between search efficiency and value signal in alpha, beta, and low gamma bands in visual epoch (100-400ms) after display onset. The same structure as Fig 5D, but for the alpha, beta, and low gamma LFP frequency bands.

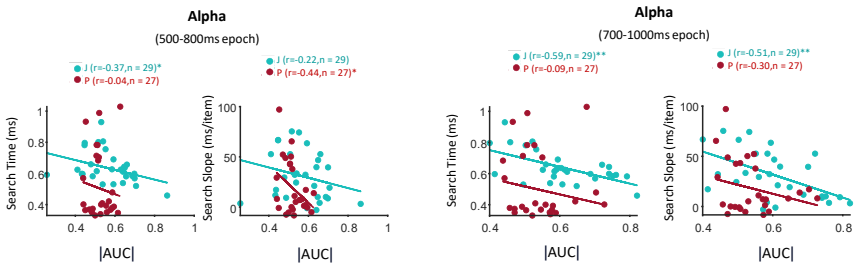

Fig S10. The correlation between search efficiency and value signal in alpha band in later periods after display onset. Similar to S9 for alpha value signal but for 500-800ms and 700-1000ms epochs.